

# Microstructural Properties and Magnetic Testing of Spot Welded Joints between Nb-Ti Filaments

G. D. Brittles, *Student Member, IEEE*, C. Aksoy, C. R. M. Grovenor, T. Bradshaw, S. Milward and S. C. Speller

**Abstract**— The production of persistent mode joints between Nb-Ti conductors remains an important problem in the field of superconducting magnets. Several researchers have demonstrated spot welding (resistance welding) as a technique capable of yielding superconducting joints directly between Nb-Ti filaments. In this study, the characteristic microstructural features associated with spot welded joints between both multifilamentary and monofilamentary Nb-Ti wires are presented. Some initial measurements of the current carrying ability of a monofilamentary joint have also been made by a novel magnetic technique. The suitability of spot welding for commercial magnet manufacture is discussed.

**Index Terms**— Spot welding, Nb-Ti joints, superconducting joint, persistent current mode, joint microstructure.

## I. INTRODUCTION

THE PRODUCTION of joints between technological superconductors with operational resistances below  $\sim 10^{-12} \Omega$  is a requirement for persistent mode (PM) magnet manufacture. Joints with much lower resistances are routinely made between Nb-Ti conductors for use in applications such as magnetic resonance imaging (MRI) scanners and nuclear magnetic resonance (NMR) spectrometers. A review of the issues surrounding PM joints between the major technological superconductors has recently been written by the authors of the present article [1].

The standard industrial jointing technique for Nb-Ti is a soldering method employing superconducting PbBi [2]. However, for environmental reasons it is timely to investigate alternative, Pb-free methods.

One such method is cold-pressing, which involves dissolving the Cu-based matrix in nitric acid and pressing together the bare filaments in a Cu or Nb-based tube [3]. However, such techniques ordinarily employ hydrofluoric acid (HF) solutions to cleanse the filament surfaces of oxides and impurities prior to jointing, which is undesirable in

commercial magnet manufacture for health and safety reasons.

Several authors have shown however that PM joints can be obtained by spot welding (otherwise known as resistance welding) bare NbTi filaments [4]–[9], including Phillip et al who found that cleaning with HF does not improve joint performance. Spot welding involves passing a high current, short duration pulse across the joint, generating resistive heat at the interfaces which is sufficient to fuse the filaments together. Alternatively the filaments can be welded to superconducting foil to increase the current carrying potential of the joint.

Spot welding thus presents a possible alternative to soldering as a Pb-free jointing technique, and has the potential for superior performance by directly bonding the Nb-Ti filaments. The major concern regarding this technique, however, is the influence of such intense heat on the carefully tailored nanostructure of the Nb-Ti material and thus on the critical current density ( $J_c$ ) and upper critical field ( $H_{c2}$ ) in the joint region.

This paper presents some initial results of a study aiming to link the superconducting properties of spot welded NbTi joints (measured by a novel magnetic technique) to their characteristic microstructural features. Section II describes the joint manufacturing techniques and characterization methods. Joint microstructural features and magnetic properties are discussed in Section III, and conclusions are made in Section IV.

## II. EXPERIMENTAL

### A. Joint manufacture

The joints presented in this work have been produced at the Rutherford Appleton Laboratory (RAL) in collaboration with the Science and Technology Facilities Council (STFC), where Nb-Ti joints are under development for a superconducting undulator magnet.

A preliminary joint (Multi1) was made between multifilamentary wires containing 24 Nb-Ti filaments of 110  $\mu\text{m}$  diameter. Firstly the Cu matrix was dissolved in 50 % aqueous nitric acid solution to reveal the filaments, and no subsequent HF cleansing was employed. The filaments were then braided together and spot welded together between 2 mm diameter Cu-alloy electrodes at several locations over a 4 cm joint length. The welding conditions were increased in intensity from the beginning to the end of the joint, varying the nominal heat setting from the minimum required to form a joint to a maximum at which the filaments were fragmented. A

This work was supported in part by the **Engineering and Physical Sciences Research Council (EPSRC)** accounts EP/K503113/1 and EP/K503769/1, and the **Tubitak International Post Doctoral Research Fellowship Programme Award #2219**.

G. D. Brittles (e-mail: [greg.brittles@materials.ox.ac.uk](mailto:greg.brittles@materials.ox.ac.uk)), C. Aksoy, C. R. M. Grovenor and S. C. Speller are with the Centre for Applied Superconductivity, University of Oxford, OX1 3PH, UK.

T. Bradshaw is with the Science and Technology Facilities Council (STFC), Rutherford Appleton Lab, OX11 0QX, UK.

S. Milward is with Diamond Light Source, Rutherford Appleton Lab, OX11 0QX, UK.

photograph of the joint is shown in Figure 1a. This wire was too large for magnetic testing, so only microstructural analysis was performed.

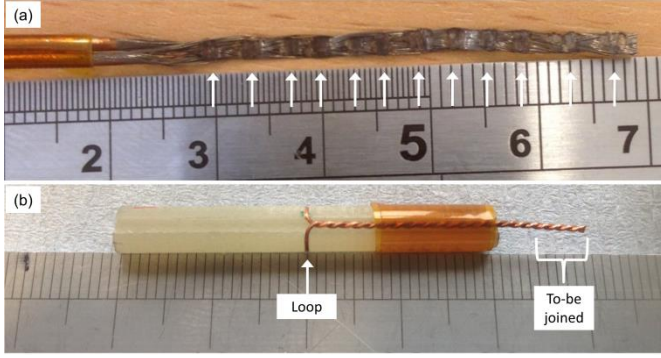


Fig. 1. (a) Joint Multi1 – filaments from two multifilamentary Nb-Ti wires exposed by etching, braided, and spot welded at locations indicated. (b) Single-turn coil wound for magnetic characterisation of joints in the MPMS (prior to jointing). Joint Mono1 was made on this coil by dissolving the Cu matrix and making 3 spot welds in the region indicated.

A second joint (Mono1) was made between monofilamentary wire (T48B-G wire from Supercon Inc.), for which the superconducting properties could be directly measured by a magnetic technique discussed in Section III. This wire contains a 200  $\mu\text{m}$  diameter Nb-Ti filament in a Cu matrix of outer diameter 0.4 mm. A single turn loop of the wire was wound into a groove on a G-10 former to a diameter  $D = 4.30 \pm 0.01$  mm between wire centres. The trailing leads were aligned parallel to the coil axis, non-inductively twisted and cut 3 cm below the loop as shown in Figure 1b. The Cu matrix was dissolved over the bottom 1 cm of the leads, causing the bare filaments to unravel. They were then re-twisted before making 3 adjacent spot welds over the bottom 6 mm, with a low heat setting on the spot welder. After initial testing, Cu was electroplated onto the joint with  $\text{CuSO}_4$  solution to improve thermal stability, as discussed further in Section III.

### B. Magnetic joint characterisation

The superconducting properties of joint Mono1 were measured with a magnetic properties measurement system (MPMS-XL7) by a novel technique discussed fully in [10] and briefly summarised here.

The coil is mounted in a standard 5 mm straw and the loop is centred in the MPMS. The coil is then zero field cooled below the 9.2 K critical temperature ( $T_c$ ) of the Nb-Ti wire to the desired measurement temperature ( $T$ ). Currents ( $I$ ) can then be induced to flow around the coil (through the joint) by changes in applied magnetic field ( $H$ ). The current in the loop produces a magnetic moment ( $\mu$ ) of approximately:

$$\mu \approx I \cdot \frac{\pi D^2}{4}, \quad [1]$$

which can be measured by DC extraction magnetometry over a 2 cm scan length, enabling the current to be calculated.

Magnetic hysteresis loops were acquired at temperatures between 4.2 and 8.0 K by sweeping the field from zero to

$+H_{max}$ , reversing down to  $-H_{max}$ , before again ramping up to  $+H_{max}$ .  $\mu(H)$  is measured in suitably small field increments of typically 0.03 to 0.10 T. These measurements are analogous to standard magnetic measurements in which the hysteresis width  $\Delta\mu(H)$  is related directly to  $J_c(H)$  [11]. Whilst a similar approach can be applied in principle to extract joint  $I_c(H)$  from hysteresis measurements on jointed coils, complications exist.

Equation 1 is strictly valid only for changes in field small enough to induce currents less than the joint  $I_c$ . Beyond this, flux begins to penetrate the loop and magnetise the inner surface of the wire, generating an additional moment contribution which is not associated with current flow through the joint. This must be subtracted in order to obtain the joint  $I_c$ . Furthermore, for the spot welded joint measured here, abnormal hysteretic behaviour discussed further in Section III complicates current flow further, preventing reliable extraction of joint  $I_c$ . Equation 1 is therefore used only to provide a first order estimate of  $I$  for a measured  $\mu$  (the secondary axis in Figure 4), but precise  $I_c$  values could not be extracted.

Joint resistance ( $R$ ) measurements were also made by the inductive resistance testing (IRT) method discussed in [10], and will not be discussed in detail here. It suffices to say that the hysteresis loops measured have an associated resistance of the order  $\sim 10^{-13} \Omega$ , and so can be considered a reasonable envelope of the PM operating regime.

### C. Sample preparation for microscopy

Following magnetic characterisation, joint Mono1 was sectioned for microscopy along with a selection of locations from Multi1. Mono1 was prepared in transverse cross section, whilst joints from Multi1 were prepared in both longitudinal and transverse cross sections.

Cross sections were prepared for scanning electron microscopy (SEM) by a standard metallographic process. Samples were held in the desired orientation by sprung steel clips, mounted in cold setting epoxy resin, ground with SiC papers down to grade #4000, polished with 6, 3 and 1  $\mu\text{m}$  diamond suspensions, and finally coated with carbon to obtain a conductive surface for SEM.

Microscopy was performed on a Zeiss Merlin SEM using an Oxford Instruments Xmax 150 mm<sup>2</sup> energy dispersive X-ray (EDX) analyser with Aztec software for chemical mapping at 10 kV.

## III. RESULTS

### A. Joint microstructures

Provided in Figure 2a is a secondary electron (SE) image of a transverse cross section through one of the higher intensity spot welds in Multi1. It is clear that spot welding overcomes surface oxides to form direct metal-metal contacts without the need for HF cleansing.

The microstructure of the transverse cross section was found to vary significantly with longitudinal position with respect to the weld centre. In regions several hundred microns from the weld centre, consolidated microstructures with macroscopically homogeneous Nb-Ti were found. In the

centre of the weld zones however, a typical spot welding microstructure was found, with a central fusion zone (FZ) and surrounding heat affected zone (HAZ) [12], as shown in Figure 2b. The FZ has a cast microstructure (shown in greater detail in Figure 2c), exhibiting coarse cored dendritic growth along the cooling gradient established by the electrodes. The dendrites are nucleated from the edge of the HAZ, which presumably remains solid. Melting in the FZ

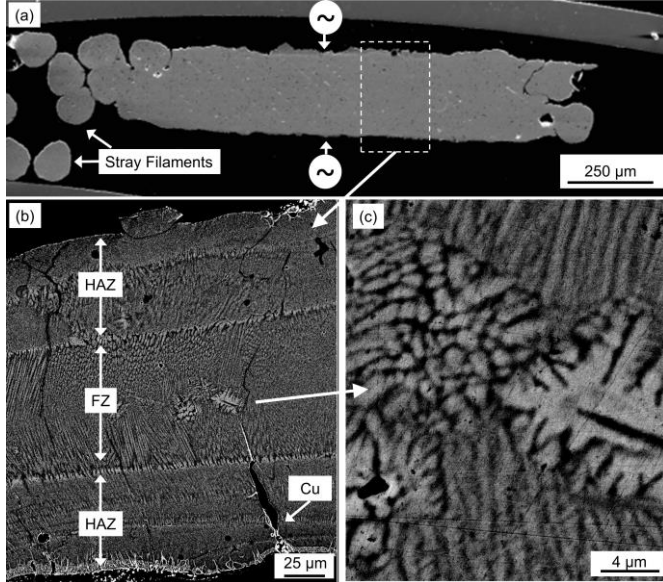


Fig. 2. Transverse cross sectional images of joint Multi1. (a) Secondary electron (SE) image demonstrating the production of an overall consolidated bulk with just a few stray filaments. The electrode pressing directions are indicated. (b) Back scattered electron (BSE) image from the region indicated in (a). The image demonstrates the large compositional inhomogeneity resulting from high temperatures produced by spot welding. The fusion zone (FZ) and heat affected zones (HAZs) are discussed in the main text. (c) Shows an expanded region from the FZ in which dendritic growth is apparent.

indicates local temperatures must reach in excess of 2000 °C. Compositional homogeneity is compromised as a result, with Ti content by weight varying from ~ 42 % in bright regions to ~ 50 % in dark regions, which is consistent with the Nb-Ti phase diagram [13]. Whilst  $H_{c2}$  may be relatively unaffected over these range of compositions, it is expected that the flux pinning nanostructure and hence  $J_c$  in this melted part of the cross section will be degraded. Cu infiltration from the electrodes of the spot welder is also apparent, but does not react widely with the Nb-Ti in this particular joint.

The microstructure of joint Mono1 shares the same basic features as Multi1, with the filaments fusing to form a single bulk as shown in Figure 3a. Microstructural modification such as in the region shown in Figure 3b does appear to be less widespread in Mono1 than Multi1 however, consuming a smaller fraction of the total cross section. This may be in part due to the lower spot welding intensity, but is also expected to be influenced by the lower density of interfaces to be joined

and thus also heat generated.

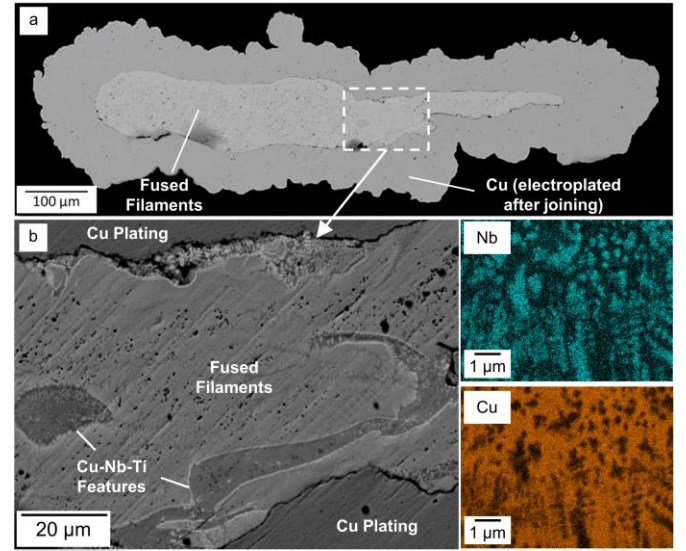


Fig. 3. (a) Transverse cross section (SE image) through one of the welds in joint Mono1. (b) BSE image from the region indicated in (a), showing Cu-Nb-Ti phases formed due to Cu infiltration during welding. These regions have a two-phase microstructure containing Nb rich dendrites in a Cu-rich matrix, as shown by EDX maps (right) taken in one such region.

The total cross sectional area of the fused filaments is ~20 % less than the sum of the two original 200 μm diameter filaments. This is likely due to slight longitudinal expansion under the compressive force of the electrodes. This alone is expected to have degraded the joint  $I_c$  by a similar fraction of the original wire  $I_c$ .

One further difference seen for joint Mono1 is that the infiltrated Cu has reacted with the molten Nb-Ti in isolated regions throughout the cross section. As is shown by EDX maps in the Figure 3, in these regions there is a two-phase Nb-Cu-Ti microstructure containing Nb-rich dendrites of composition ~55/20/25 wt.% in a Cu-rich matrix of composition ~13/60/27 wt.%. These phases are expected to have poor superconducting properties and degrade joint performance.

### B. Joint superconducting properties

Figure 4a shows full  $\mu$ - $H$  hysteresis loops measured for the coil containing joint Mono1. Flux jumping occurs regularly at lower temperatures, which is due in part to the impaired thermal stability in the joint region caused by removal of the matrix. Cu was later electroplated onto the joint, which significantly reduced but did not altogether eliminate flux jumping. In general however, poor thermal stability is to be expected in this test setup due to the relatively low cooling power supplied by He gas in the MPMS, the insulating G-10 sample holder, and the large Nb-Ti filament diameter. Similar behaviour is seen for soldered and cold pressed joints which have also been tested by this method.

Measurement analysis is therefore focussed on higher temperature measurements (predominantly 8 K, as shown in Figure 4b), where flux jumping does not occur. Also shown in the figure are two curves associated with the Nb-Ti wire itself. The first (dotted line) is  $\mu$ - $H$  data measured for the coil prior to jointing (an open coil), which provides the zero-current



baseline for joint measurements. The second is the Nb-Ti wire  $I_c$  (dashed line), measured by a standard magnetic method and scaled to  $I_c$  values provided by the manufacturer. This provides the upper limit on joint performance.

The measured moment of the jointed coil exceeds the baseline over the entire field range, demonstrating a non-zero joint  $I_c$ . Although the applied field was unfortunately reversed prior to closure of the hysteresis loop, it is clear by comparison with the wire  $I_c(H)$  that the joint has a similar  $H_{c2}$  to that of the wire (2.6 T at 8.0 K). It can therefore be inferred that current paths through high  $H_{c2}$  Nb-Ti material exist in the joint, which is consistent with the microstructure.

The shape of the hysteresis loop in Figure 4b is deformed compared to that commonly found for PbBi soldered joints, having a low field peak effect and asymmetry about both the  $\mu = 0$  and  $H = 0$  axes. Unusual behaviour upon reversal of the applied field is also found.

These features are symptomatic of incomplete flux penetration, which is commonly seen in magnetic measurements made on Nb-Ti wires in longitudinal applied fields due to large longitudinal screening currents [14]. With the joint held longitudinally in the measurements made here, it

is thought that similar behaviour may prevent full flux penetration of the joint in this case.

In light of these effects, joint  $I_c$  measurements cannot be extracted from the hysteresis loops. Repeating the measurements with the joint held perpendicular to the applied field may alleviate these problems and allow for a more complete analysis. Anisotropy of joint  $I_c$  should also be considered.

#### IV. CONCLUSIONS

Microstructural analysis of spot welded joints between both multifilamentary and monofilamentary Nb-Ti filaments has revealed characteristic features associated with this joining technique. Spot welding produces complete metallurgical bonds between oxidised filaments and hence a consolidated joint. Whilst in peripheries of the weld there is excellent bonding with little microstructural inhomogeneity, in other regions temperatures exceed 2000°C and melt the NbTi, dramatically modifying the microstructure. Cu was also found to infiltrate from the electrodes, in some regions reacting with the Nb-Ti to form a two-phase Nb-Cu-Ti microstructure.

Magnetic characterisation of a monofilamentary joint demonstrates that the joints contain superconducting current paths with  $H_{c2}$  similar if not equal to that of the Nb-Ti wire itself. However, due to what appears to be incomplete flux penetration, full joint  $I_c(H, T)$  data could not be extracted from the loops, and must be addressed in further work.

It is evident that spot welding can produce excellent joints capable of performing in high background fields and employing neither leaded components nor HF treatments. It is not yet clear however whether the microstructural modifications found here can be controlled by modifying processing conditions, nor whether a repeatable process can be established on the production line. The safety of this method should also be considered when used to join very fine filament wires, given their flammability and the possibility of arcing between the spot welding electrodes, which occurred commonly in this investigation

#### ACKNOWLEDGMENT

The authors are grateful for the assistance of C. Lockett in joint manufacture, as well as D. Prabhakaran and A. Boothroyd of The Clarendon Laboratory for use of the MPMS.

#### REFERENCES

- [1] G. D. Brittles, T. Mousavi, C. R. M. Grovenor, C. Aksoy, and S. C. Speller, "Persistent current joints between technological superconductors," *Supercond. Sci. Technol.*, vol. 28, p. 093001, Aug. 2015.
- [2] R. F. Thornton, "Superconducting joint for superconducting wires and coils," U.S. Patent 4 744 506, May 17, 1988.
- [3] J. Liu, J. Cheng, and Q. Wang, "Evaluation of NbTi Superconducting Joints for 400 MHz NMR Magnet," *IEEE Trans. Appl. Supercond.*, vol. 23, pp. 34-39, Dec. 2013.
- [4] E. Karvonen and J. M. Rayroux, "Electrical connection between superconductors," U.S. Patent 3 527 876, Sept 8, 1970.

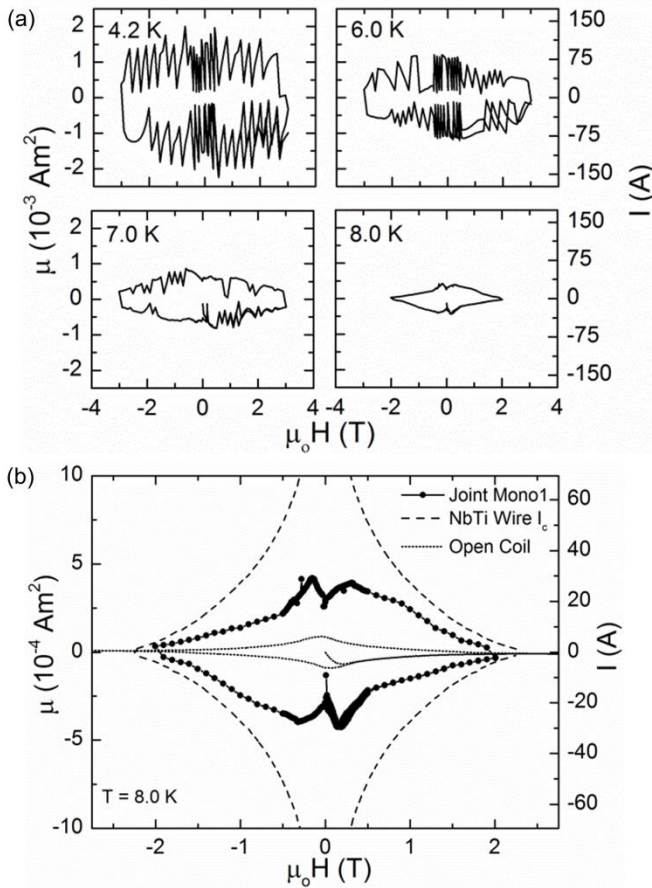


Fig. 4. Magnetic moment ( $\mu$ ) versus applied magnetic field  $\mu_0 H$  hysteresis loops measured for the coil closed with joint Mono1. (a) Loops obtained at temperatures from 4.2 to 8.0 K. Flux jumping occurs regularly at lower temperatures. The secondary axis shows current values calculated from Equation 1, which are only approximate for reasons discussed in Section II. (b) The 8 K hysteresis loop plotted alongside the open coil baseline (dotted line), and Nb-Ti wire  $I_c$ . The low field features and asymmetry of the loop are thought to be caused by incomplete flux penetration, as discussed in the main text.

- [5] G. Luderer, P. Dullenkopf, and G. Laukien, "Superconducting joint between multifilamentary wires," *Cryogenics*, vol. 14, pp. 518-519, Sept. 1974.
- [6] J. E. C. Williams, S. Pourrahimi, Y. Iwasa, L. J. Neuringer, and L. Motowidlo, "600 MHz spectrometer magnet," *IEEE Trans. Magn.*, vol. 25, pp. 1767-1770, Mar. 1989.
- [7] T. Tominaka, S. Kakugawa, N. Hara, and N. Maki, "Electrical properties of superconducting joint between composite conductors," *IEEE Trans. Magn.*, vol. 27, pp. 1846-1849, Mar. 1991.
- [8] S. Phillip, J. V. Porto, and J. M. Parpia, "Two methods of fabricating reliable superconducting joints with multifilamentary Nb-Ti superconducting wire," *J. Low. Temp. Phys.*, vol. 101, pp. 581-585, Nov. 1995.
- [9] D. G. Blair, H. Paik, and R. C. Taber, "How to make high critical current joints in Ni-Ti wire," *Rev. Sci. Instrum.*, vol. 46, Aug. 1975.
- [10] G. D. Brittles, P. Noonan, S. A. Keys, C. R. M. Grovenor, and S. Speller, "Rapid characterisation of persistent current joints by SQUID magnetometry," *Supercond. Sci. Technol.*, vol. 27, p. 122002, Nov. 2014.
- [11] C. P. Bean, "Magnetization of High-Field Superconductors," *Reviews of Modern Physics*, vol. 36, pp. 31-39, Jan. 1964.
- [12] N. Charde, "Effects of Electrode Deformation of Resistance Spot Welding on 304 Austenitic Stainless Steel Weld Geometry," *J. Mech. Eng. Sci.*, vol. 3, pp. 261-270, Dec. 2012.
- [13] L. Cooley, P. Lee, and D. C. Larbalestier, "Conductor processing of low Tc materials: the alloy NbTi" in *Handbook of Superconducting Materials Vol. 1*. Bristol, UK: IoP Pub. 2003, ch. B3.3.2, pp. 603-638
- [14] A. P. Martinelli and B. Turck, "Some effects of field orientation on the magnetization of superconducting wires," *Cryogenics*, vol. 18, pp. 155-161, Mar. 1978.